Supplemental Material – Shear-induced phase transition and critical exponents in 3D fiber networks

Sadjad Arzash,[1,2] Jordan L. Shivers,[1,2] and Fred C. MacKintosh[1,2,3]

[1] *Department of Chemical & Biomolecular Engineering, Rice University, Houston, TX 77005*
[2] *Center for Theoretical Biological Physics, Rice University, Houston, TX 77030*
[3] *Departments of Chemistry and Physics & Astronomy, Rice University, Houston, TX 77005*

Distribution of the critical strain γ_c

The critical strain γ_c for every individual sample is identified in the absence of fiber bending rigidity $\kappa = 0$ as the strain where the shear stress becomes finite. Using the bisection method, we are able to approach γ_c from above with high precision [1, 2]. The distribution of these values are shown in Fig. S1 for the models we used in this paper. The critical strain depends on the network's connectivity z as well as its architecture. As expected, for networks with larger z the critical strain is smaller. We also note that as the system size increases the network becomes more isotropic, thus the width of γ_c distribution becomes smaller [3].

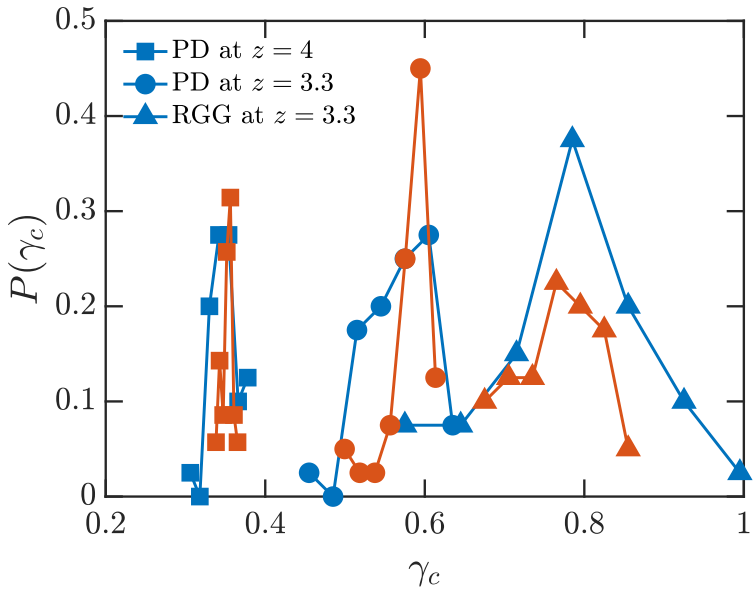

FIG. S1. The distribution of the critical strain γ_c for various network models used in this study, as shown in the legend. The blue and red colors correspond to the network's lateral size of $W = 16$ and $W = 25$, respectively. As can be observed, by increasing the system size, the distribution becomes narrower.

Fitting procedure for finding the critical exponents f and ϕ

To obtain the scaling exponent f, we use the modulus data at $\kappa = 0$ that are beyond the finite-size dominated regime, i.e., we use the data that satisfy $W \gtrsim \xi$ or equivalently $|\Delta\gamma| \times W^{1/\nu} \gtrsim 1$. On the other end, for strains far above the critical point, clearly the networks are outside the critical regime. This effect can be seen as a deviation of the power law behavior. Moreover, we only fit our exponents for the largest system size, where this intermediate regime is largest. Since $K - K_c \sim |\gamma - \gamma_c|^f$, we first compute the log of $K - K_c$ and $\gamma - \gamma_c$ and then we use the linear fit function in the Curve Fitting package of MATLAB to find the exponent f, which is the slope of our fit. This is done for every individual sample to obtain the full distribution for the exponent f. We report the standard deviation of this distribution as the error for f. We recognize, however, that this is almost certainly an underestimate of the real error.

The exponent ϕ, on the other hand, is found by using the modulus data at finite bending rigidity $\kappa > 0$. We use the data corresponding to $\kappa = 10^{-5}$. Since below the critical strain, we expect that $K \sim \kappa|\gamma - \gamma_c|^{f-\phi}$ for networks with finite κ, similar to the fitting procedure for finding f, we first compute the log of K and $|\gamma - \gamma_c|$ for the data that satisfy $|\Delta\gamma| \times W^{1/\nu} \gtrsim 1$, then by performing a linear fit we find the slope $f - \phi$ for every individual sample. Note that the exponent f is already known from the central force data, thus we are able to obtain the exponent ϕ for every sample. We use the mean value of f for obtaining ϕ exponents. We report the standard deviation of the distribution of ϕ values as the error.

3D PD networks at $z = 3.3$

In this section, we present the finite-size analysis of the shear modulus discontinuity K_c (Fig. S2) as well as the unscaled data for the differential nonaffinity $\delta\Gamma$ (Fig. S3) for 3D PD networks at $z = 3.3$. As it can be observed in Fig. S2, we find a decreasing trend of K_c as the system size W increases, in agreement with prior work in 2D [2, 4].

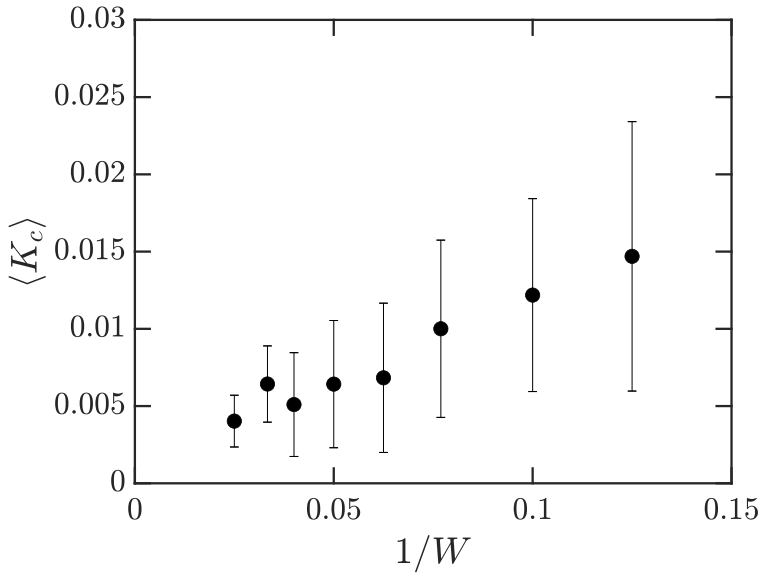

FIG. S2. The ensemble average of shear modulus discontinuity K_c for 3D PD networks at $z = 3.3$ versus the inverse of system size $1/W$. Similar to 2D networks, we find that K_c decreases as we increase W. However, due to large finite-size effects, our data are not inconsistent with a vanishing K_c in the thermodynamic limit.

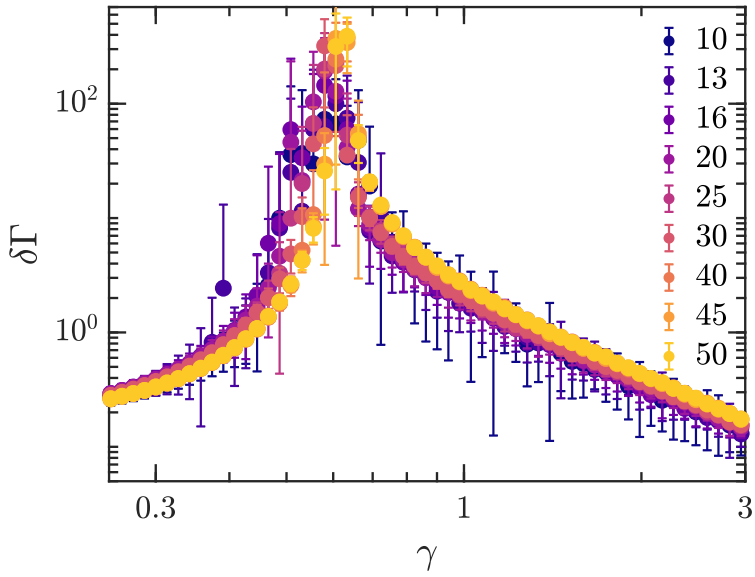

FIG. S3. The differential nonaffinity parameter versus shear strain for 3D PD networks at $z = 3.3$ for different system sizes as indicated in the legend. The finite-size scaling analysis of these data is shown in the main text.

3D RGG networks at $z = 3.3$

To construct random geometric graph (RGG) networks [5], we place $N = W^3$ nodes with random positions in a periodic box of sided length W. We then iterate through all pairs of nodes, connecting nodes separated by distance ℓ_{ij} according to a log-normal probability distribution $P(\ell_{ij})$, such that $\ln(\ell_{ij})$ is normally distributed with mean $\mu = \ln(\ell_0)$ and variance $\sigma = 0.5$. The probability of connecting two nodes separated by distance ℓ_{ij} is

$$P(\ell_{ij}) = \begin{cases} 0 & \text{for } \ell_{ij} < \ell_{\min} \text{ or } \ell_{ij} > \ell_{\max} \\ A(z)\exp(-(\ln(\ell_{ij}/\ell_0)^2/(2\sigma^2)) & \text{for } \ell_{\min} \le \ell_{ij} \le \ell_{\max} \end{cases} \tag{1}$$

in which $\ell_{\min} = \ell_0/2$, $\ell_{\max} = 3\ell_0$, and the prefactor $A(z)$ is chosen so that the average connectivity of the final network is z. A sample bond length probability distribution for a network with size $W = 20$ and connectivity $z = 3.3$ is shown in Fig. S4.

We note that the RGG model contains longer bonds than PD networks. As a result, for small system sizes, it is possible for small connected clusters of nearly aligned bonds to span the length of the simulation box. These clusters, which may comprise only a small fraction of the network's bonds, nonetheless determine the critical strain at which the K becomes nonzero. As a result, in some cases, such networks exhibit an apparent two-branch behavior, with a regime of unusually low stiffness immediately above the critical strain followed by a more typical stiffening regime at larger strains. Similar behavior has been observed in 2D triangular networks [2]. We demonstrate this effect for a set of RGG network samples in Fig. S5. To calculate f for RGG networks, we removed samples exhibiting this two-branch behavior from our ensemble. Since the shear modulus for the samples with a two-branch behavior cannot be fit as a power law. Figure S6 b shows the finite-size scaling analysis of K for the RGG model at $z = 3.3$ after removing these samples.

The finite-size analysis of the shear modulus discontinuity K_c for the RGG model is shown in Fig. S7. Similar to the 3D PD model, we observe a decreasing trend of K_c as W increases. Figure S8 shows the behavior of the RGG model with finite bending rigidity as well as a Widom-like collapse of the data using the obtained scaling exponents. The unscaled differential nonaffinity parameter of this model at zero bending rigidity for different sizes is shown in Fig. S9.

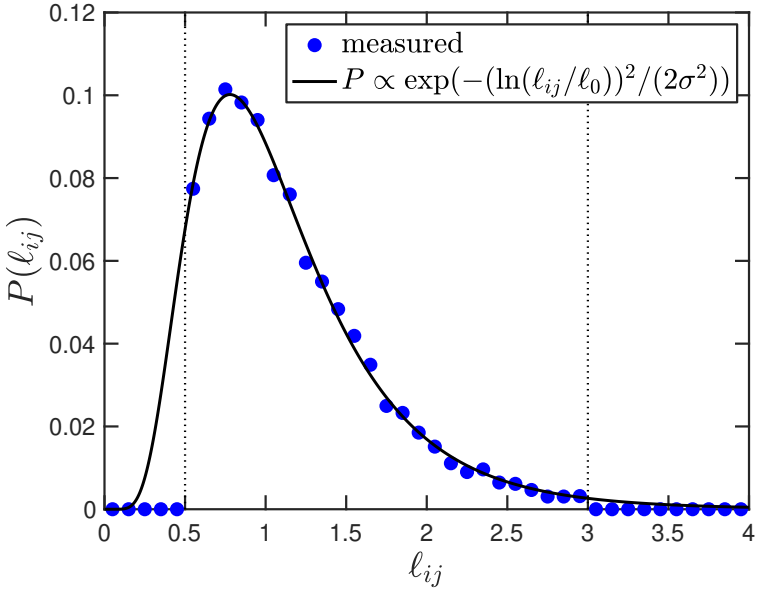

FIG. S4. Bond length probability distribution for an RGG network of side length $W = 20$ and connectivity $z = 3.3$.

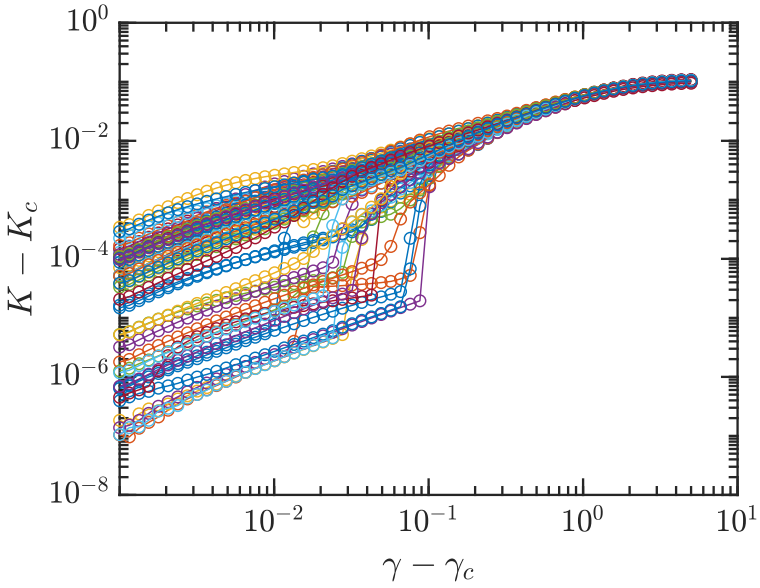

FIG. S5. The excess shear modulus versus the excess shear strain for 40 random samples of RGG networks at $z = 3.3$ and $W = 25$. A significant number of samples exhibit a two-branch behavior, an artifact of this specific geometry at small sizes.

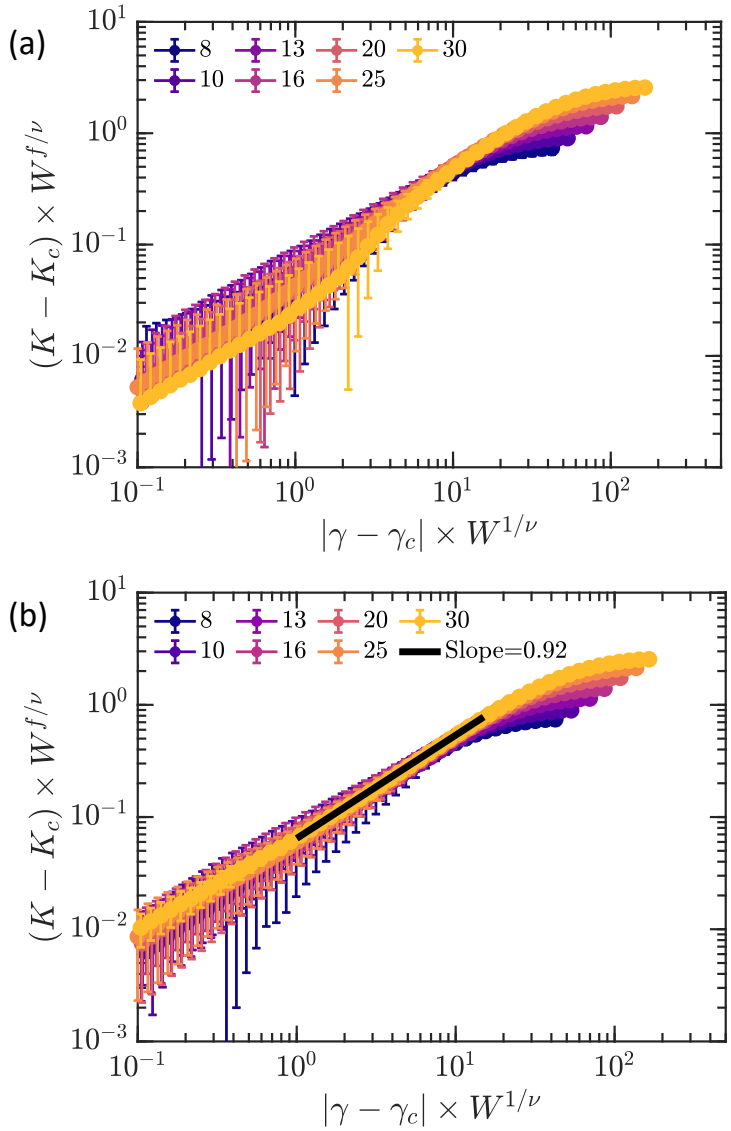

FIG. S6. The finite-size scaling analysis of the RGG model at $z = 3.3$. (a) Showing the analysis by including all samples. (b) The analysis after removing the random samples that exhibit two-branch behavior. We find an $f = 0.92 \pm 0.02$ by averaging 5 samples of size $W = 30$. We used $\nu = (f + 2)/3$.

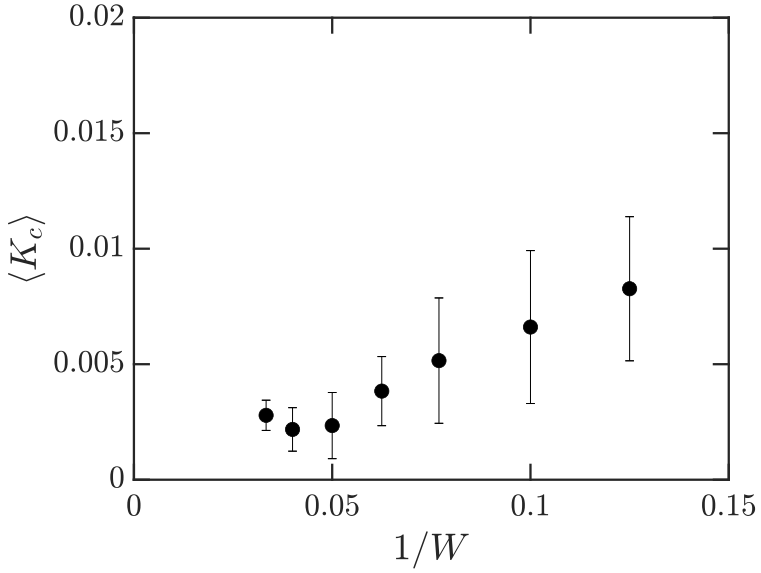

FIG. S7. The ensemble average of shear modulus discontinuity K_c for 3D RGG networks at $z = 3.3$ versus the inverse of system size $1/W$. Similar to 2D networks, we find that K_c decreases as we increase W. However, due to large finite-size effects, our data are not inconsistent with a vanishing K_c in the thermodynamic limit.

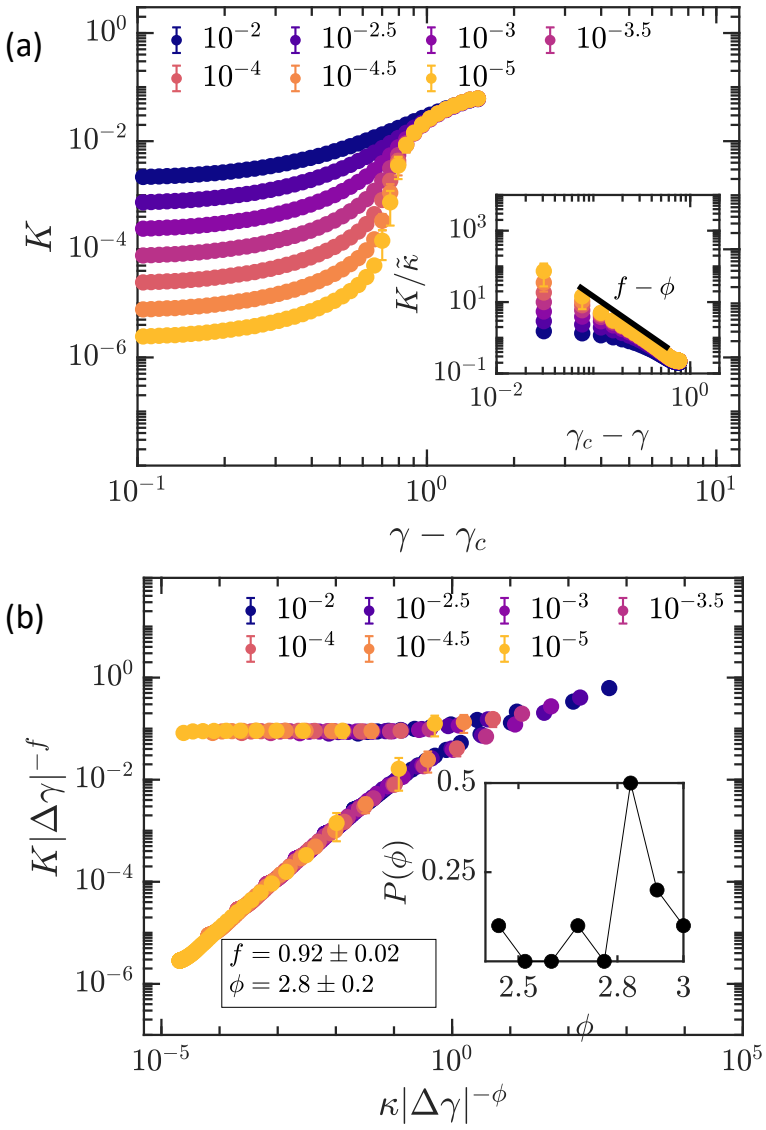

FIG. S8. (a) Differential shear modulus K for RGG networks with $z = 3.3$ and system size $W = 30$ at various bending stiffness κ as shown in the legend. The inset shows the scaling behavior of K in the subcritical region, where $K \sim \kappa|\gamma - \gamma_c|^{-\lambda}$ with $\lambda = \phi - f$. (b) A Widom-like scaling collapse of the data in (a). The inset shows the distribution of the scaling exponent ϕ.

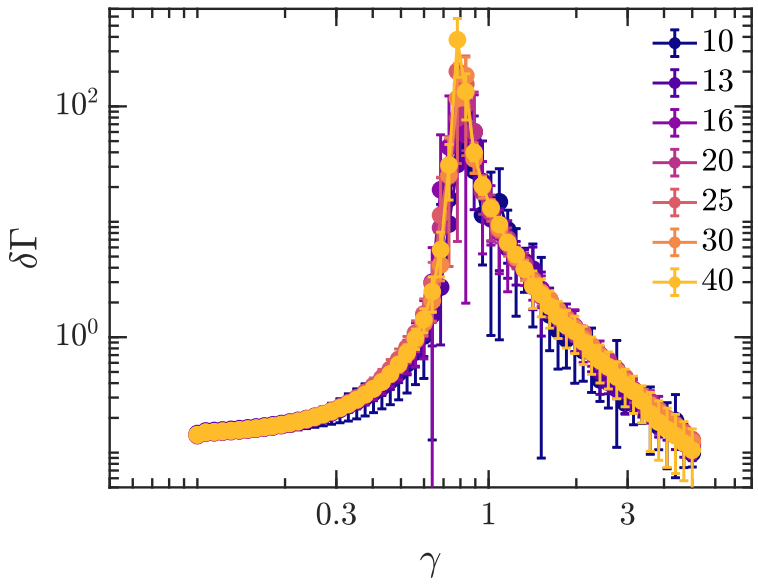

FIG. S9. The differential nonaffinity parameter versus shear strain for 3D RGG networks at $z = 3.3$ for different system sizes as indicated in the legend. The finite-size scaling analysis of these data is shown in the main text.

3D PD networks at $z = 4.0$

The following figures are showing the same analysis that has been performed in the main text for a different network connectivity $z = 4.0$. The scaling exponents are close to what we obtained for networks at $z = 3.3$. These data again confirm that the scaling relation $f = d\nu - 2$ works in 3D. For all of the following figures, the data are obtained by averaging 40 random realizations.

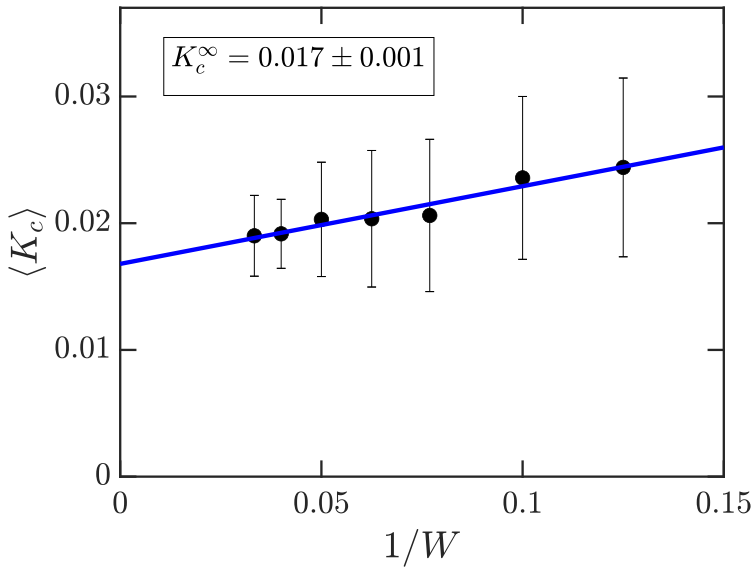

FIG. S10. The ensemble average of shear modulus discontinuity K_c versus the inverse of system size $1/W$ for 3D PD networks at $z = 4.0$. Similar to 2D networks, we find that K_c decreases as we increase W. By fitting a linear equation to the data (shown as a solid blue line), we find a small intercept of 0.017 that is the shear modulus discontinuity in the thermodynamic limit.

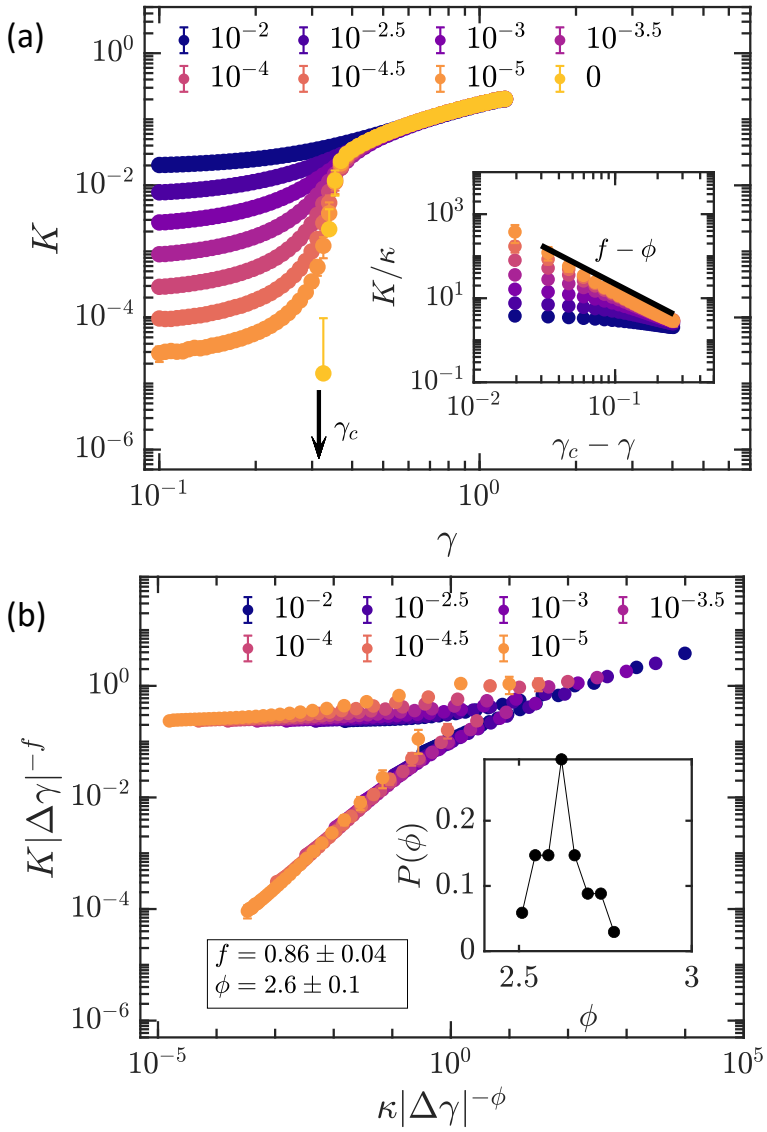

FIG. S11. (a) The differential shear modulus of 3D PD networks at $z = 4.0$ with size $W = 30$ for different values of bending stiffness between bonds κ, as shown in the legend. As discussed in the main text, in the subcritical regime $\gamma < \gamma_c$ we expect $K \sim \kappa|\gamma - \gamma_c|^{f-\phi}$. This has been plotted in the inset, f has been already obtained from the finite-size scaling plot of the central-force networks and we find $\phi = 2.6 \pm 0.1$ using the data at $\kappa = 10^{-5}$. (b) A Widom-like scaling collapse of the data in (a). The inset shows the distribution of the scaling exponent ϕ.

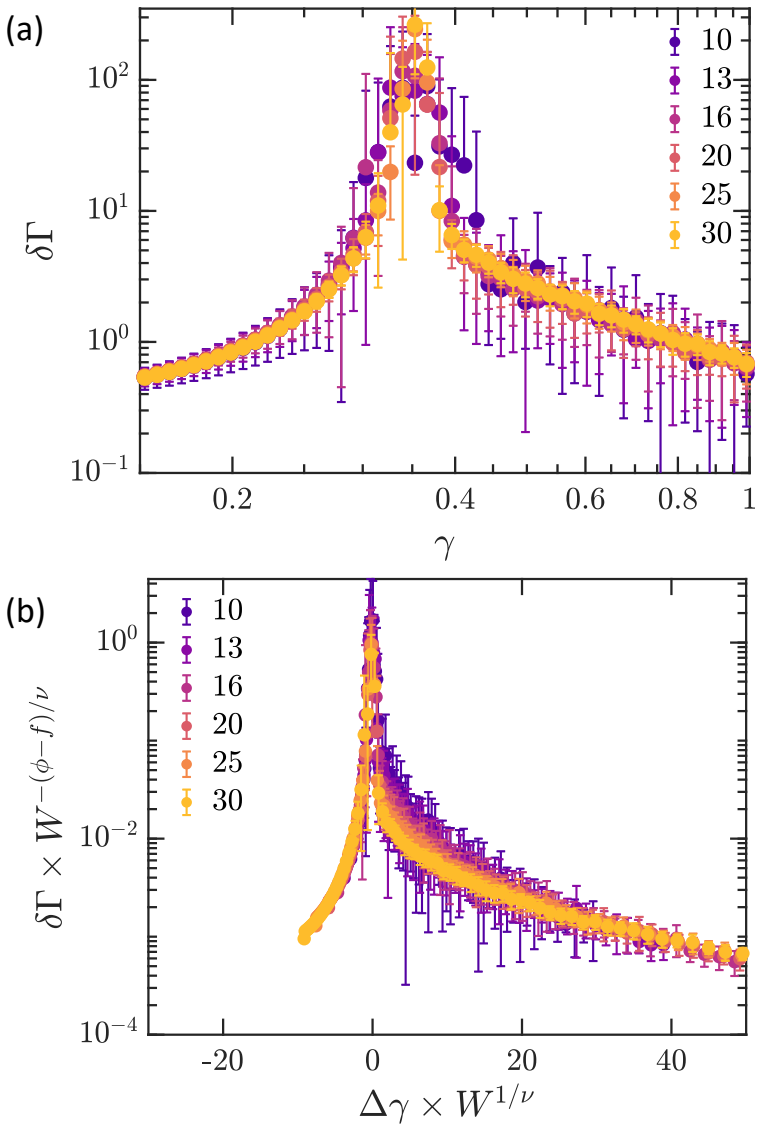

FIG. S12. (a) The differential nonaffinity parameter for various network sizes as shown in the legend for 3D PD networks at $z = 4.0$. (b) The finite-size scaling collapse of the data in (a). The scaling exponents f and ϕ have been already obtained. The correlation length exponent ν, however, is calculated using the hyperscaling relation $f = d\nu - 2$, which results in $\nu = 0.95$. This great collapse of nonaffine fluctuations confirms again that the hyperscaling relation holds in 3D networks.

The effect of the shear direction

All the presented results of this study are obtained by shearing the networks in x direction in the $x-z$ plane. However, an important question can be asked about other shear directions and if different shear directions will give different critical exponents. We address this question by shearing the networks in three different directions and compare our findings. As can be seen from simulations of both PD and RGG networks at $z = 3.3$ and at a system size of $W = 16$, various shear directions exhibit similar behavior (Fig. S13). This shows that the shear modulus K in our network models behave isotropically even at a small size of $W = 16$. We also note that the two-branch behavior is observed in all shear directions in the RGG model.

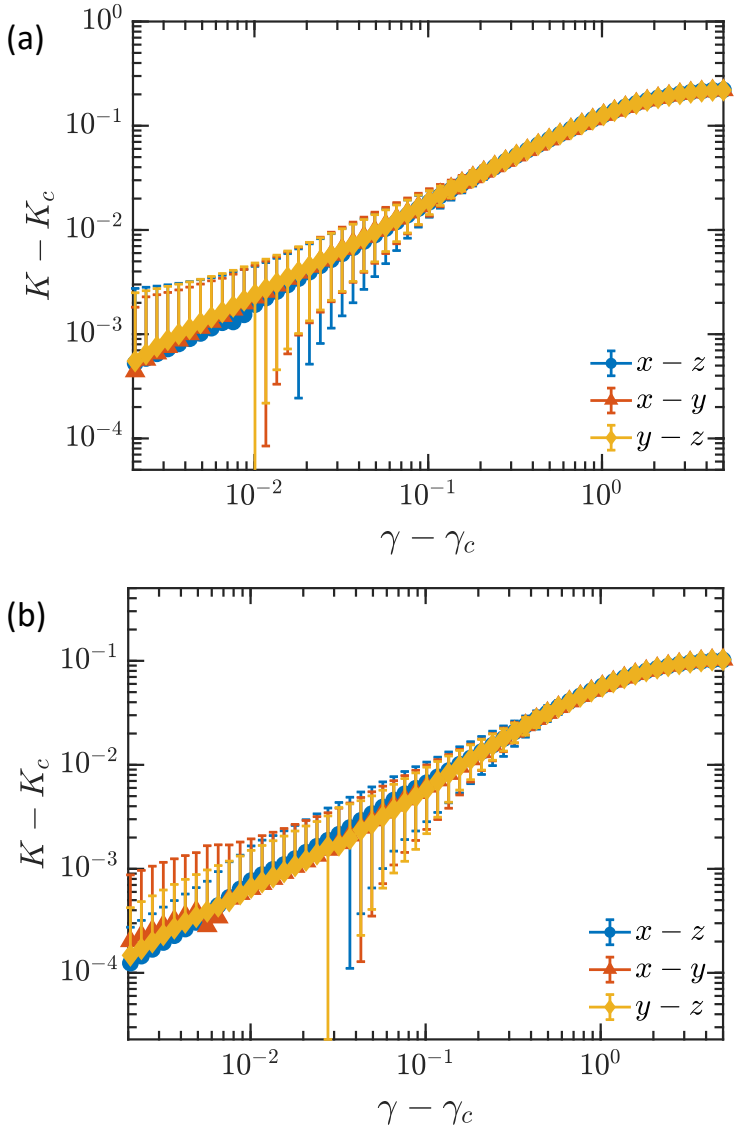

FIG. S13. The behavior of shear modulus in various shear directions as indicated in the legend for (a) 3D PD model at $z = 3.3$ and a system size $W = 16$ averaged over 40 random samples (b) 3D RGG model with the same z, W and number of random samples.

[1] M. Merkel, K. Baumgarten, B. P. Tighe, and M. L. Manning, Proceedings of the National Academy of Sciences **116**, 6560 (2019).
[2] S. Arzash, J. L. Shivers, and F. C. MacKintosh, Soft Matter **16**, 6784 (2020).
[3] J. L. Shivers, S. Arzash, A. Sharma, and F. C. MacKintosh, Physical Review Letters **122**, 188003 (2019).
[4] M. F. J. Vermeulen, A. Bose, C. Storm, and W. G. Ellenbroek, Physical Review E **96**, 053003 (2017).
[5] F. Beroz, L. M. Jawerth, S. Münster, D. A. Weitz, C. P. Broedersz, and N. S. Wingreen, Nature Communications **8**, 16096 (2017).